Pulsed laser induced ohmic back contact in CdTe solar cells

Brian J. Simonds, Vasilios Palekis, Brian Van Devener, Christos Ferekides, and Michael A. Scarpulla

Citation: Applied Physics Letters **104**, 141604 (2014); doi: 10.1063/1.4870838
View online: http://dx.doi.org/10.1063/1.4870838
View Table of Contents: http://scitation.aip.org/content/aip/journal/apl/104/14?ver=pdfcov
Published by the AIP Publishing

Pulsed laser induced ohmic back contact in CdTe solar cells

Brian J. Simonds,[1,a)] Vasilios Palekis,[2] Brian Van Devener,[3] Christos Ferekides,[2] and Michael A. Scarpulla[1,4]
[1]*Materials Science and Engineering, University of Utah, Salt Lake City, Utah 84112, USA*
[2]*Electrical Engineering, University of South Florida, Tampa, Florida 33620, USA*
[3]*University of Utah, Salt Lake City, Utah 84112, USA*
[4]*Electrical and Computer Engineering, University of Utah, Salt Lake City, Utah 84112, USA*

(Received 22 January 2014; accepted 28 March 2014; published online 8 April 2014)

Creating an ohmic back contact has long been a problem for making efficient CdTe solar cells. Current devices utilize some combination of preferential chemical etching, buffer layer, and Cu doping with additional cost, time, and complexity added for each step. In this Letter, these processes are eschewed and replaced with a nanosecond pulsed ultraviolet laser treatment. It is shown that this treatment can eliminate the rollover effect seen in photovoltaic current-voltage (J-V) curves that is indicative of a non-ohmic back contact. Transfer length measurements show that a single UV laser pulse can reduce the specific contact resistivity by a factor of 24 versus untreated samples. X-Ray photoemission spectroscopy shows evidence of increased conductivity and of elemental Te created at the surface by laser pulses. Finally, finite element modeling is used to model the laser-sample interaction, which predicts both the temperature and the amounts of Cd and Te lost during a laser pulse. © *2014 AIP Publishing LLC*. [http://dx.doi.org/10.1063/1.4870838]

A well-known challenge in making CdTe solar cells is the formation of an ohmic back contact. The large electron affinity and p-type doping of CdTe result in difficulty finding a metal with a sufficiently large work function. Unless special surface preparations are applied before the conductive back contact layer is added, a Schottky diode of reverse polarity to the CdS/CdTe junction results.[1] This problem is compounded by the fact that CdTe allows for only modest doping levels due to self-compensation meaning that in some cases the depletion widths of the front and back contacts overlap. This results in a decreased electron barrier at the back contact with a resulting loss in open circuit voltage (V_{oc}). A feature indicative of a poor back contact is seen in the first quadrant of a photovoltaic device's J-V curve, where the current saturates with applied voltage and a "rollover" betrays a loss of V_{oc} as well as fill factor (FF).[2] Several engineering methods have been devised to circumvent this problem, many of which have been reviewed elsewhere.[3] Most of these include a selective etching process to produce a Te-rich surface to form a p^+ layer combined with the deposition of a buffer layer and the addition of Cu before adding the current carrying metallic layer. The purpose of the p^+ layer is to facilitate efficient hole tunneling at the back contact. Presented here is evidence that pulsed nanosecond ultraviolet (UV) laser treatments can be used to create the Te-rich layer at the interface between CdTe and a metallic back contact that greatly reduces the contact resistivity as well as eliminates the rollover effect increasing V_{oc} and FF.

The laser-material interactions for nanosecond lasers occur under conditions of thermal equilibrium between the photogenerated carriers and the lattice. A ns pulsed laser creates a Te-rich layer by exploiting the large difference in vapor pressure between Cd and Te at high temperatures. A shallow penetrating (high photon energy) laser pulse very rapidly heats the surface causing preferential evaporation of Cd as it is the more volatile species. Brewer *et al.*[4] were the first to show this effect in crystalline CdTe, and several other groups have studied the effects of pulsed UV lasers on c-CdTe and its alloys.[5–7] This method was first applied to polycrystalline CdTe by Nelson *et al.*[8] where high spatial resolution X-Ray photoemission spectroscopy (XPS) microscopy was used to measure a Te enrichment at the surface of an ultrahigh vacuum (UHV) sublimated CdTe thin film that had not been exposed to ambient. In this Letter, the concept was extended to polycrystalline CdTe films used for photovoltaics and was demonstrated as part of the fabrication of photovoltaic devices.

It was possible to predict and quantify the Te enrichment at the surface of CdTe due to pulsed UV laser exposure. This was done by calculating the time dependent surface temperatures reached during the pulse, which was accomplished by developing a 3-dimensional, finite element model constructed with the COMSOL Multiphysics platform. Thin film CdTe samples were prepared by a close-space sublimation process whereby several microns of film were deposited on alumina substrates. The laser anneals were carried out by a KrF excimer laser emitting 248 nm pulses of about 25 ns duration. Multiple pulsed anneals were done with a 10 Hz repetition rate (which is long enough for the sample to cool between pulses). A 5×5 mm^2 aperture was used that was much smaller than the size of the beam so that the spatial profile of the beam was assumed to be approximately flat. In order to study the surface chemistry of the laser annealed samples, XPS was performed on a Kratos Axis Ultra DLD system using a monochromatic Al x-ray source. To eliminate the effects of surface oxides and adventitious carbon on the interpretation of XPS data, the following procedure was utilized. First, the as-deposited sample was placed in the UHV XPS chamber where a brief (60-90 s) 4 keV Ar-ion etch was applied until no carbon or oxygen signal was detected by a

[a)]Author to whom correspondence should be addressed. Electronic mail: Brian.Simonds@utah.edu

broad energy, low resolution (pass energy = 160 eV) scan. During high resolution (pass energy = 40 eV) scans, some C and O was detected but it was reduced by more than an order of magnitude from the as-deposited sample. Then the sample was transferred from the UHV chamber via a sealed transfer device to an argon filled glove bag where the sample was mounted in a laser annealing chamber. The chamber consisted of stainless steel walls with a UV transmitting quartz window and sealed with KF vacuum flanges so that the samples were annealed in an inert Ar environment. After laser treatment, the sample was returned to the UHV XPS chamber by reversing the above steps so that the sample is never directly contacted by an ambient environment. To account for charging at the surface during the XPS measurement, the system's charge neutralizer apparatus was used.

Direct measurements of the changes in the back contact resistance were measured by the transfer length method (TLM).[9] TLM devices were constructed by depositing 300 $\times$ 500 μm^2 molybdenum contact pads on the 5 μm thick CdTe, whose long sides were separated by a range of gap spacings. Isolation of the test region from adjacent areas of the film was achieved by creating a channel around the set of TLM pads by focused ion-beam etching. The total resistance was calculated from the measured current obtained for sweeping voltage across two neighboring pads from $\pm$1 V. The effect of the changes in back contact resistance on solar cell device performance was tested by applying the laser treatments to complete solar cell stacks minus the back contact. These samples were typical superstrate devices (TCO/CdS/CdTe) with fabrication details found elsewhere.[10] After deposition of the absorber, they were laser treated followed by the application of a Mo-based back contact. As opposed to the samples prepared for XPS analysis, the devices made for TLM and solar cell measurements were annealed in air.

In order to investigate the effects of ns UV laser pulses on thin film CdTe, a finite element model was developed that combined the optical absorption processes with heat generation and transport. A detailed discussion of this model and the temperature profiles can be found in a previous publication.[11] In brief, the model considered a 1 $\times$ 1 mm^2, 25 ns, 248 nm laser pulse incident on a 5 μm thick CdTe film on an alumina substrate. Light absorption at 248 nm, obeying the Beer-Lambert law, gives a penetration depth of about 9 nm with an absorption coefficient of 10^6 cm^{-1}. Because of this shallow penetration, the thickness of the substrate was found to be irrelevant to the outcome of the predicted temperatures. Boundary conditions include surface-to-ambient infrared radiation, room temperature convection, and heat loss due to evaporation of Cd and Te from the surface.[12] This last condition is proportional to $(\Lambda_{Cd}J_{Cd}(T) + \Lambda_{Te}J_{Te}(T))$ where Λ is the latent heat of vaporization. The quantity $J(T)$ is the temperature dependent mass flux of atoms defined as

$$J(T) = p(T)\sqrt{M/(2\pi kT)}, \quad (1)$$

where $p(T)$ is the vapor pressure of a particular species, M is the mass, and k is the Boltzmann factor.

The result of a temperature versus time simulation at the surface of a CdTe film for a 50 mJ/cm^2 pulse is given in Figure 1(a). The dashed line represents the laser pulse input

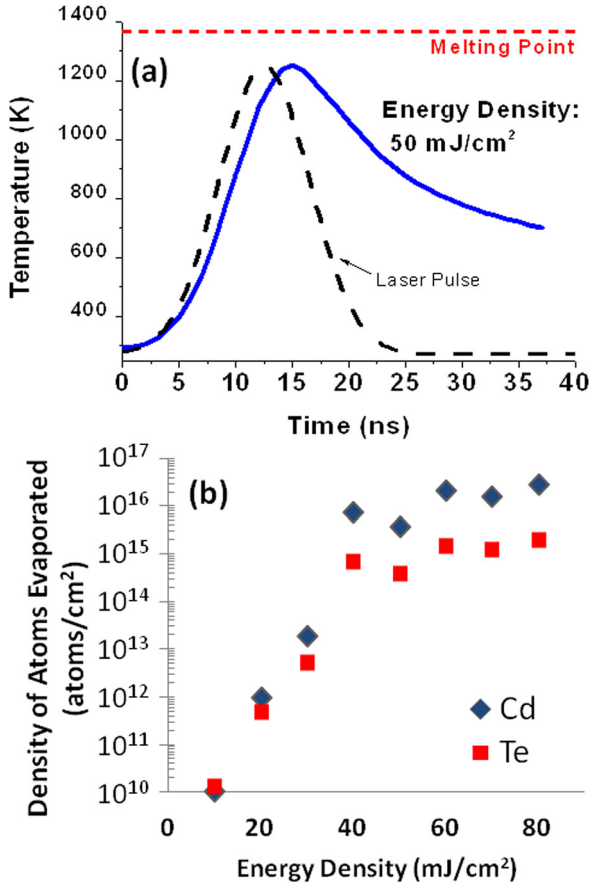

FIG. 1. (a) Predicted temperature versus time at the front surface of the CdTe film (blue). The dashed line is a normalized profile of the simulated laser pulse and the horizontal dotted line (red) is the melting point of CdTe. (b) The calculated areal density of Cd and Te atoms leaving the surface resulting from a single laser pulse.

used in the simulation and the horizontal line at 1365 K gives the melting point of CdTe. In addition to showing that very high temperatures can be rapidly achieved, this plot can be used to calculate the amount of Cd and Te lost during laser heating due to evaporation. By inserting the calculated T(t) into Eq. (1), one gets $J(T(t))$ that was then integrated to give the total mass of a particular species lost during the laser pulse. Figure 1(b) shows the computed values of the densities of Cd and Te atoms lost during single pulses. From these data, it is seen that by 40 mJ/cm^2 there is an order of magnitude more Cd lost from the surface than Te and that this differential evaporation ratio becomes relatively constant with increasing laser fluences. This is a direct result of the non-linearity of the evaporation boundary condition. At higher temperatures, it causes the maximum surface temperature to increase much more slowly with increasing pulse energy. It is assumed that the Te-enrichment predicted by this model scales linearly with the number of pulses. The model predicts that the surface reaches the melting point around 80 mJ/cm^2. This was investigated with scanning electron microscopy (SEM) which showed no noticeable changes to the film surface until roughly this fluence. The film thickness was not significantly changed from these laser treatments. The SEM images of the effects of laser treatments on the morphology of our film can be seen in a previous publication.[11]

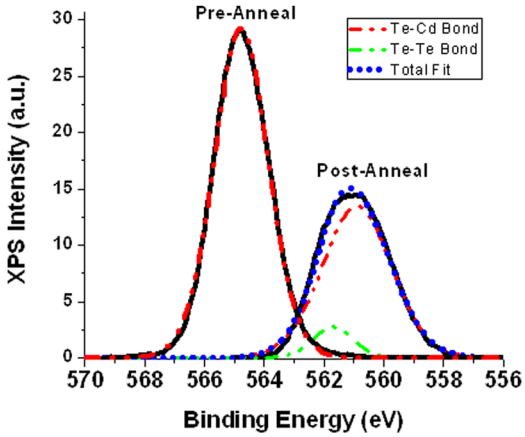

FIG. 2. Experimental curves (black solid) for the Te $3d_{5/2}$ from pre and post laser treatment. The pre-anneal data are fit by a single line shape representing Te-Cd bonds (red dash dot). The post-anneal data are fit by an additional smaller peak from metallic Te (green dash dot) with the total fit shown as the solid (blue dotted) line.

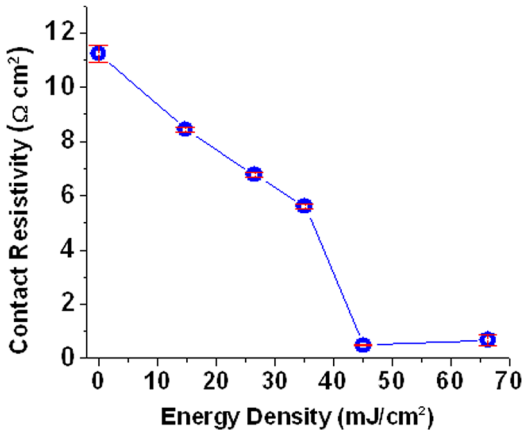

FIG. 3. Contact resistivity as a function of energy density from TLM measurements of samples treated with single laser pulses.

XPS data and analysis are shown in Figure 2 for the Te $3d_{5/2}$ peak for a sample annealed at 65 mJ/cm^2 for 600 pulses. These parameters were chosen as 65 mJ/cm^2 is predicted by our model (see Figure 1(b)) to produce a large difference in Cd versus Te evaporation and is well below the melting threshold. The large number of pulses was used to enhance this effect, making detection easier. The untreated sample shows a peak centered near 565 eV binding energy and the laser treated sample shows one at 561 eV. The data were analyzed by first subtracting a Shirley background then by fitting using a Marquardt algorithm to a Voigt line shape with 30% Guassian and 70% Lorentzian character. The as-deposited sample is fit well by a single line shape and is identified as arising from Te bonded to Cd.[13] The laser treated sample is asymmetrically broadened as well as shifted towards lower binding energy. The asymmetry in this peak can be accounted for by including a second curve shifted 0.8 eV to higher binding energy than the main one, which is the predicted location of the elemental Te signal.[14] The presence of both phases is similar to results of Te layers deposited by vacuum deposition[15] and those created by chemical etching.[16] The shift of the main peak to lower binding energy is due to the surface becoming more conductive as a result of laser treatments. This was confirmed by monitoring the C 1s peak before and after laser treatment where a 3.2 eV shift was seen that is compared to a 3.1 eV shift of the main Te $3d_{5/2}$ peak. This difference is negligible within the resolution limit of the XPS system and analysis.

The specific contact resistivity determined from TLM measurements is shown in Figure 3 for single pulses at various energy fluences. The contact resistivity is lowered most dramatically at and above 45 mJ/cm^2 where it is almost 24 times lower than the as-deposited sample. The large drop in contact resistivity between 35 and 45 mJ/cm^2 is consistent with the predictions of Figure 1(b) that the differential ratio of Cd to Te evaporation occurs at and above 40 mJ/cm^2. The next highest energy density tested did not decrease the contact resistivity further but instead gave a small increase. The small increase is close to the experimental error but could be a result of the onset of laser induced damage to the film. Also, from the predictions made in Figure 1(b), it was expected that the differential amounts of evaporated Cd and Te not increase drastically after about 40 mJ/cm^2.

Figure 4 shows the effects of UV laser treatment on solar cell device performance as it compares a sample with no surface treatment versus ones that were laser treated with 50 mJ/cm^2 for 10 and 100 pulses. The untreated sample clearly shows the rollover effect due to a non-ohmic contact. After 10 pulses, however, this effect is starting to diminish and is completely gone by 100 pulses. Additionally, both the FF and the V_{oc} of the 100 pulse sample improve markedly over the untreated case. This is clear evidence that the laser-induced Te enrichment at the surface, which lowered the contact resistivity, creates an ohmic back contact translating directly to improved device performance. Devices made with 500 and 1000 pulses showed some degradation in solar cell performance that could be due to laser induced surface damage. Further work is necessary to determine the optimum number of pulses for device performance.

The effect of multiple pulses is difficult to predict with the model used above as the model assumes as a starting point a stoichiometric CdTe surface, which is only strictly true for the first pulse as every subsequent pulse will see an

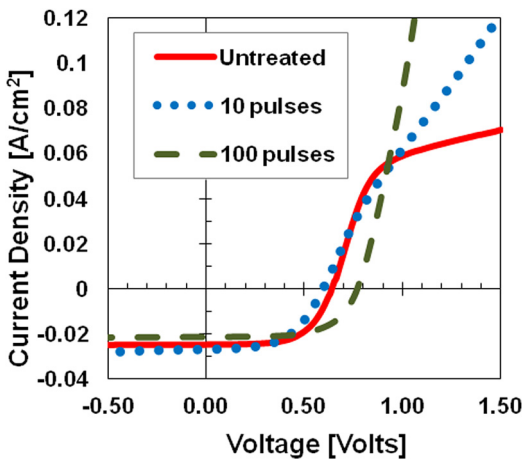

FIG. 4. J-V measurements of solar cell devices made with and without a laser induced back contact junction. Laser treatments were performed at 50 mJ/cm^2.

increasingly Te-rich surface. Additionally, the model does not take into account the effects of surface topography or grain boundaries. It has been shown that following a UV laser pulse that Te enrichment occurs at the grain boundaries with Cd enrichment at the grain hillocks.[8] If a similar situation is assumed here then the grain boundaries are becoming more p-type and the surfaces of the individual grains becoming less p-type. Therefore, the increase in conductivity we see in Figure 3 and the improved ohmic contact seen in Figure 4 would be dominated by the stoichiometry changes at the surfaces of the grain boundaries. Evidence of elemental Cd was looked for in the XPS results but the separation of the elemental Cd peak and the Cd-Te peak is only 0.1 eV,[14] which was too small to be detected by our apparatus.

The effects of UV pulsed laser treatments on the surfaces of p-CdTe and on the back contact junction of p-CdTe solar cells have been presented. Finite element modeling of the Cd and Te loss during the laser pulse predicted a substantial Te enhancement during a single 25 ns laser pulse. Evidence of this enhancement was seen in XPS data, which revealed an elemental Te phase as well as a more conductive surface following laser annealing. The contact resistance was measured directly by TLM that showed more than an order of magnitude decrease in the specific contact resistivity over the laser fluences measured. Finally, solar cells were fabricated utilizing a UV pulsed laser annealed back contact. These results showed improvement in FF, V_{oc}, and J_{sc} as well as eventually being able to eliminate the rollover effect that is indicative of a non-ohmic back contact.

This work was supported in full by the Department of Energy through the Bay Area Photovoltaic Consortium under Award No. DE-EE0004946. The FIB instrument is part of the University of Utah USTAR shared facilities supported, in part, by the MRSEC Program of the NSF under Award No. DMR-1121252. The XPS instrument is part of the University of Utah shared facilities of the Micron Microscopy Suite sponsored by the College of Engineering, Health Sciences Center, Office of the Vice President for Research, and the Utah Science Technology and Research (USTAR) initiative of the State of Utah. Finally, we greatly appreciate the use of the excimer laser facilities of Professor Ashutosh Tiwari at the University of Utah.

[1]G. Stollwerck and J. R. Sites, in *Proceedings of 13th European PVSEC, Nice, France* (1995), p. 2020.
[2]S. H. Demtsu and J. R. Sites, Thin Solid Films **510**, 320 (2006).
[3]B. E. McCandless and J. R. Sites, in *Handbook of Photovoltaic Science and Engineering*, 2nd ed., edited by A. Luque and S. Hegedus (John Wiley and Sons, Ltd., Chichester, 2011), p. 622.
[4]P. D. Brewer, J. J. Zinck, and G. L. Olson, Appl. Phys. Lett. **57**, 2526 (1990).
[5]L. A. Golovan, P. K. Kashkarov, Yu. N. Sosnovskikh, V. Yu. Timoshenko, and V. M. Lukeenkov, Phys. Solid State **40**, 187 (1998).
[6]Y. Hatanaka, M. Niraula, Y. Aoki, T. Aoki, and Y. Nakanishi, Appl. Surf. Sci. **142**, 227 (1999).
[7]V. A. Gnatyuk, T. Aoki, Y. Nakanishi, and Y. Hatanaka, Surf. Sci. **542**, 142 (2003).
[8]A. J. Nelson, M. Nanailov, L. Gregoratti, M. Marsi, and M. Kiskinova, J. Appl. Phys. **87**, 3520 (2000).
[9]D. K. Schroder, *Semiconductor Material and Device Characterization*, 3rd ed. (John Wiley and Sons, Inc., Hoboken, 2006), p. 146.
[10]C. Ferekides, D. Marinskim, V. Viswanathan, B. Tetali, V. Palekis, P. Selvaraj, and D. L. Morel, Thin Solid Films **361–362**, 520 (2000).
[11]B. J. Simonds, V. Palekis, M. I. Khan, C. S. Ferekides, and M. A. Scarpulla, Proc. SPIE **8826**, 882607 (2013).
[12]L. A. Golovan, B. A. Markov, P. K. Kashkarov, and V. Yu. Timoshenko, Solid State Commun. **108**, 707 (1998).
[13]T. S. Sun, S. P. Buchner, and N. E. Byer, J. Vac. Sci. Technol. **17**, 1067 (1980).
[14]J. F. Moulder, W. F. Stickle, P. E. Sobol, and K. D. Bomben, in *Handbook of X-ray Photoelectron Spectroscopy*, edited by J. Chastain (Perkin-Elmer Corporation, Eden Prarie, MN, 1992), p. 131.
[15]D. W. Niles, X. Li, P. Sheldon, and H. Höchst, J. Appl. Phys. **77**, 4489 (1995).
[16]D. Kraft, A. Thissen, J. Broetz, S. Flege, M. Campo, A. Klein, and W. Jaegermann, J. Appl. Phys. **94**, 3589 (2003).